Astron. Astrophys. 339, 591–600 (1998)

ASTRONOMY
AND
ASTROPHYSICS

# The dust extinction, polarization and emission in the high-latitude cloud toward HD 210121

**Aigen Li**[1,2] **and J. Mayo Greenberg**[1]

[1] Leiden Observatory Laboratory, Leiden Observatory, Postbus 9504, 2300 RA Leiden, The Netherlands
[2] Beijing Astronomical Observatory, Chinese Academy of Sciences, Beijing 100101, P.R. China

Received 14 April 1998 / Accepted 27 August 1998

**Abstract.** The interstellar extinction, polarization and emission in the high-latitude cloud toward HD 210121 have been explored in terms of a four-component core-mantle interstellar dust model. We assume that the dust content in this cloud is of Galactic plane origin and has been lifted to its current position either by some sort of (particle) destructive violent energetic expulsion ("Galactic fountain"), or by the relatively gentle "photolevitation", or some combination of these two. The polarization curve, peaking at a smaller wavelength than the Galactic average, is well fitted by the core-mantle particles with thinner mantles than for the average interstellar dust as would have resulted from partial erosion of the Galactic plane core-mantle particles. In modeling the extinction curve, an extra component of small silicates resulting from the destruction of the "laid-bare" core-mantle particles is added to account for the FUV extinction together with PAH's. The sum of the four dust components (core-mantle, hump, PAH's and small silicates) can be made to closely match the extinction curve which is characterized by an extremely steep FUV rise. The dust IR emission spectrum has also been calculated for radiation fields with various intensity. Comparison of the model calculation with the IRAS data suggests that the radiation field is weaker than the average interstellar radiation field in the diffuse Galactic interstellar medium. For comparison, attempts have also been made to fit the extinction on the basis of the silicate/graphite (+PAH's) model. While the core-mantle model and the silicate/graphite+PAH's model are consistent with the *solar* abundance constraint, the silicate/graphite model needs an unrealistically high silicon depletion to account for the FUV extinction. If the interstellar medium abundance is only $2/3$ of the solar abundance, all models would face the problem of an abundance budget crisis using the standard dust/gas ratio. However, due to the uncertainty of the hydrogen column density, the actual dust/gas ratio may be different from the standard value. Thus the abundance constraint may not be as serious as it appears.

**Key words:** ISM: dust, extinction – polarization – ISM: abundances – stars: individual: HD 210121 – ultraviolet: ISM – infrared: ISM: continuum

*Send offprint requests to*: A. Li

## 1. Introduction

The interstellar dust content in high-latitude clouds (HLCs) has been the subject of considerable attention not only because it provides information on the spatial variation of the chemical and physical properties of interstellar dust, but also because, to some extent, it reflects the cloud's history and present environment (radiation field, shocks, magnetic field etc). Dust also plays an important role in the photon/chemical processes in interstellar clouds and thus the knowledge of the dust properties is essential for the studies of the interstellar cloud chemistry for which HLCs provide one of the best testing grounds. The cirrus cloud toward HD 210121 (a B3V background star), discovered by de Vries & van Dishoeck (1988) and identified as DBB 80 in the IRAS 100 $\mu$m emission survey (Désert et al. 1988), is one of the most extensively studied high latitude clouds. This cloud is located at $(l, b) \sim (57^o, -45^o)$ with a vertical distance of $\approx 104\,\mathrm{pc}$ from the Galactic plane [Gredel et al. 1992; but also see Welty & Fowler (1992) who suggest $\approx 150\,\mathrm{pc}$]. Observations of this line of sight covered various wavelength bands ranging from ultraviolet (UV), optical, infrared (IR) to (sub)millimeter and radio (Heiles & Habing 1974; Désert et al. 1988; de Vries & van Dishoeck 1988; Welty & Fowler 1992; Gredel et al. 1992; Stark & van Dishoeck 1994; Larson et al. 1996; Stark et al., in preparation). With respect to its relatively low visual extinction ($\mathrm{A_v} \simeq 1\,\mathrm{mag}$, comparable to the classical diffuse cloud $\zeta$ Oph), the molecular abundances in this cloud are rather high and are more characteristic of dark clouds (de Vries & van Dishoeck 1988; Gredel et al. 1992; Welty & Fowler 1992; Stark & van Dishoeck 1994). The well-determined molecular abundances are of particular interest for understanding the physical and chemical structure of high-latitude clouds through interstellar cloud chemistry modeling and in turn, provide tests on models (see e.g., van Dishoeck & Black 1988, van Dishoeck & Black 1989). In chemical modeling, the dust extinction and scattering properties and the elemental depletion are needed as input parameters (see van Dishoeck 1994 for a review). The main purpose of this work is to quantitatively constrain the dust properties in the HD 210121 cloud so as to more competely understand the environment and the physical characteristics of this cloud. The recent optical and near-infrared (NIR) polarimetric and the NIR photometric measurements (Larson et al. 1996) with the addition of the UV extinction curve (Welty & Fowler 1992) are used as an observational basis for our dust model.

In Sect. 2 we discuss the possible dust components in terms of the core-mantle interstellar dust model, assuming that the HD 210121 cloud dust is of Galactic plane origin but has been subjected to destructive processes. The polarization is calculated in Sect. 3 so as to infer the nature of the large core-mantle grains. In Sect. 4 the extinction curve is modeled on the basis of the four-dust-component core-mantle model. For comparison, we have also modeled the extinction in Sect. 5 in terms of the silicate/graphite model as well as the modified silicate/graphite model with an addition of a PAH's component. The elemental depletions are discussed for the core-mantle model and for the silicate/graphite (+PAH's) model. Sect. 6 presents the predicted dust infrared emission spectrum calculated from the core-mantle model and its implication for the strength of the interstellar radiation field in this high-latitude cloud. Discussions are presented in Sect. 7 followed by a concluding summary in Sect. 8.

## 2. Dust components: observational evidences

In contrast to clouds in the Galactic plane average, the interstellar polarization curve for the line of sight toward HD 210121 peaks at $\lambda_{\rm max} \approx 0.38\,\mu{\rm m}$ (Larson et al. 1996). As $\lambda_{\rm max}$ is proportional to the grain size (Greenberg 1968), the HD 210121 cloud dust is considerably smaller than that of the diffuse Galactic interstellar medium where $\lambda_{\rm max}$, on average, is about $0.55\,\mu{\rm m}$. Furthermore, the extinction curve for this line of sight is characterized by an extremely steep far ultraviolet (FUV) rise and by a relatively weak and broader 2200 Å hump (Welty & Fowler 1992). This clearly indicates that very small particles which are responsible for the FUV extinction are unusually rich in comparison with the Galactic average. It is interesting to note that a steeper FUV rise for the high-latitude cloud dust than the average Galactic value was predicted in modeling the average high-latitude cirrus spectrum (Dwek et al. 1997). In addition, the ratio of the IRAS $12\,\mu{\rm m}$ emission to the $100\,\mu{\rm m}$ emission, ${\rm I}(12\,\mu{\rm m})/{\rm I}(100\,\mu{\rm m})$, of this cloud is higher by a factor of 2–3 than that of the typical diffuse interstellar medium (Welty & Fowler 1992). Since the $12\,\mu{\rm m}$ emission is attributed to the stochastic heating of very small particles, this also implies that very small particles are enhanced in the HD 210121 cloud.

For the diffuse clouds in the Galactic plane, on the basis of grain cyclic evolution, a tri-modal interstellar dust model has been developed: large silicate core-organic refractory mantle dust particles; very small carbonaceous particles responsible for the hump extinction; and PAH's responsible for the FUV extinction (Greenberg 1978; Hong & Greenberg 1980; Li & Greenberg 1997). However, the origin and evolution of the dust components of HLCs are not yet known, although the existence of dust at high galactic latitudes has been known for a long time (see e.g. Shane & Wirtanen 1967, de Vaucouleurs & Buta 1983). On the one hand, it is well established that supernova explosions can expel dust and gas from the Galactic plane ("Galactic fountain"). On the other hand, it has also been suggested that small dusty clouds can be raised to high Galactic latitudes by radiation pressure (Franco et al. 1991). Here we propose a model for the HD 210121 cloud by assuming that the dust grains in this cloud originated in the Galactic plane and were raised most likely by the violent "Galactic fountain" explosion process, although the relatively gentle "photolevitation" mechanism is not excluded as making an extra contribution. We thus expect that the core-mantle particles in the HD 210121 cloud should be smaller than their Galactic plane counterparts since they could have been partially eroded during the expulsion process. We also expect a component of small silicate particles because a fraction of the core-mantle grains could even have been destroyed or fragmented into small pieces. This scenario is qualitatively consistent with the above-mentioned observations for the smaller peak wavelength $\lambda_{\rm max}$ and the steep FUV extinction rise indicating decrease in size of the tenth micron particles as well as enhanced numbers of very small particles. Summarized then, there could be four dust components in the high latitude cloud toward HD 210121: silicate core-organic refractory mantle dust particles; small silicate particles; very small carbonaceous hump particles; and PAH's. Finally, although the dust layer in the Galaxy has a thickness of about $120\,{\rm pc}$ (Deul & Burton 1992), the variations of the IR intensities near the HD 210121 region and the large brightness (Welty & Fowler 1992) support that the dust contents seen in this line of sight are not local.

## 3. Polarization

The detection of interstellar polarization tells us that the dust grains (at least some) in the line of sight cloud toward HD 210121 must be non-spherical and aligned. It is reasonable to assume that the core-mantle grains, exclusively, contribute to the observed polarization and assume that small silicates, hump particles and PAH's are either spherical or not well-aligned since smaller grains are less efficiently aligned and no 2200 Å polarization was detected for the general diffuse interstellar medium.

For simplicity, we model the core-mantle grains as infinite cylinders. Following our earlier work on the Galactic average (Li & Greenberg 1997), the size distribution is taken to be ${\rm n(a)} \sim \exp\,[-5\,(\frac{\rm a-a_c}{\rm a_i})^2]$, where ${\rm a}$, ${\rm a_c}$, ${\rm a_i}$ are the radius of the core-mantle dust grain, the radius of the silicate core, and the cut-off size of the distribution, respectively. The average radius is $<{\rm a}>= {\rm a_c} + 0.252\,{\rm a_i}$. Note that ${\rm n(a)}$ is actually the distribution of the mantle thickness, while ${\rm a_c}$ is kept as a constant, representing the average size of the silicate core. In this work, the radius of the silicate core is taken as the same as the Galactic plane value, ${\rm a_c} = 0.042\,\mu{\rm m}$ (Li & Greenberg 1997), because the silicate core (of those particles which are still coated) has been shielded by the organic refractory mantle. Therefore, there is only one free parameter left in modeling the polarization curve: ${\rm a_i}$. The optical constants of silicates and organic refractories are taken from Li & Greenberg (1997). Adjusting the cut-off size ${\rm a_i}$ and assuming perfect spinning alignment, we find that the polarization curve is best fitted by ${\rm a_i} = 0.056\,\mu{\rm m}$ which corresponds to (by coincidence) an average radius $<{\rm a}>= 0.056\,\mu{\rm m}$. For the Galactic average, the best fit is given by ${\rm a_i} = 0.080\,\mu{\rm m}$

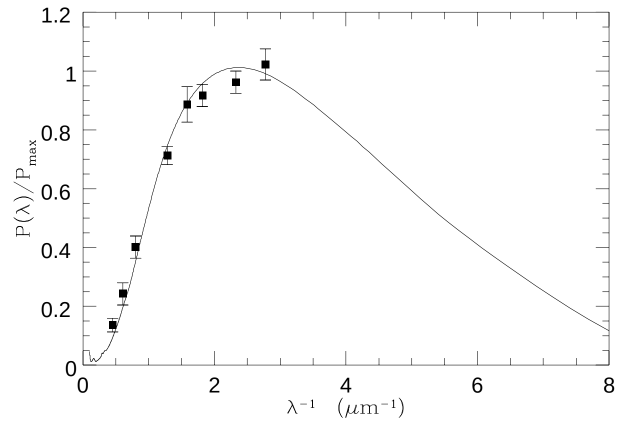


**Fig. 1.** The silicate core-organic refractory mantle dust particles (solid line) fits to the interstellar polarization curve of the high-latitude cloud toward HD 210121 (squares with error bars; Larson et al. 1996). The dust size distribution is $\mathrm{n(a)} \sim \exp{[-5\,(\frac{\mathrm{a-a_c}}{\mathrm{a_i}})^2]}$ with $\mathrm{a_c} = 0.042\,\mu\mathrm{m}$ and $\mathrm{a_i} = 0.056\,\mu\mathrm{m}$.

with a corresponding average radius $<\mathrm{a}>= 0.062\,\mu\mathrm{m}$ (Fig. 4 in Li & Greenberg 1997). This quantitatively shows that the HD 210121 cloud grains are relatively smaller than those in the Galactic plane; i.e., with thinner mantles. Fig. 1 presents the calculated polarization curve as well as the observational data. Unfortunately, there is insufficient polarimetric observational data for $\lambda^{-1} > 3\,\mu\mathrm{m}^{-1}$. Future observations at shorter wavelengths would provide a useful test on the core-mantle dust model.

## 4. Extinction

### *4.1. The extinction curve*

The extinction is a sum of the contributions of four dust components. The contribution from the core-mantle component can be easily obtained because the parameters for the core-mantle grains have already been determined through fitting the polarization curve. The thin solid line in Fig. 2 shows the theoretical extinction curve calculated from the core-mantle particles. It can be clearly seen in Fig. 2 that the infrared, visual, near-ultraviolet extinction, similar to the Galactic average case, are dominated by the contribution of the core-mantle component.

In spite of various attempts made to investigate the 2200 Å hump carrier (hump particles), its nature still remains unknown. No existing analogs are able to satisfy the major observational constraint of a very stable hump peak position but with large variations in the hump width along sight lines of different environment. Mennella et al. (1996) reported that a stable peak position can be obtained by subjecting small hydrogenated amorphous carbon (HAC) grains to UV radiation, although the laboratory produced humps are too wide and too weak with respect to the interstellar one. Most recently, Rouleau et al. (1997) proposed that the effects of particle shape and particle clustering as well as the intrinsic particle chemical composition could account for the hump width variability. On the basis of such theoretical expectations, Schnaiter et al. (1998) performed experimental investigations and confirmed that the hump width is indeed strongly influenced by the particle shape and the clustering degree. They suggested that isolated nano-sized carbon grains could serve as a real dust analog for the hump carrier. We are not going to explore the hump particle material in detail but just assume that it is some form of carbonaceous material. The optical properties of hump particles are here described by a Drude profile with a peak position at $4.6\,\mu\mathrm{m}^{-1}$ and a width $1.09\,\mu\mathrm{m}^{-1}$ (Welty & Fowler 1992) for the hump region $\lambda \leq 0.5\,\mu\mathrm{m}$. Note that the hump of the Galactic average extinction curve peaks at the same position but with a somewhat narrower width $1.0\,\mu\mathrm{m}^{-1}$ (see Fitzpatrick & Massa 1986, Désert et al. 1990). If one attempts to attribute the larger hump width to a higher particle clustering degree, it is difficult to understand why the general size distribution tends to be smaller than the Galactic average. For $\lambda \geq 0.5\,\mu\mathrm{m}$, the carbonaceous hump particle extinction is calculated using the graphite optical constants of Draine & Lee (1984).

For PAH's, we adopt the absorption cross sections summarized in an analytical formula by Désert et al. (1990) which was obtained by subtracting the large (core-mantle) particle and the hump component from the curvature of the extinction curve in the FUV. We should note that the FUV absorption properties of PAH's are not well known. The uncertainty in the PAH's FUV cross sections would result in significant uncertainty in deriving the PAH's carbon abundance which depends inversely on the adopted PAH's FUV absorption properties. Allamandola et al. (1989) estimated the FUV cross sections per carbon atom of PAH's to be $3 \times 10^{-18} - 2 \times 10^{-17}\,\mathrm{cm}^2$. Joblin et al. (1992) measured the FUV cross section of a 31-carbon-atom PAH to be $\approx 6 \times 10^{-18}\,\mathrm{cm}^2$ per carbon atom at $\lambda^{-1} = 8\,\mu\mathrm{m}^{-1}$. The analytical approximation adopted here (Désert et al. 1990) gives $\approx 1 \times 10^{-17}\,\mathrm{cm}^2$ per carbon atom at $\lambda^{-1} = 8\,\mu\mathrm{m}^{-1}$ which is intermediate between the other estimates.

The size distributions for hump particles and PAH's are more flexible than for the core-mantle particles because the extinction efficiencies (i.e. the Drude function for hump particles and the analytical formula for PAH's) are not sensitive to grain size in the size ranges considered here. Thus we adopt for the HD 210121 cloud the size distributions as derived for the Galactic average: $\mathrm{n(a)} \propto \mathrm{a}^{-3}$, $\mathrm{a} \in [15,\, 120]$ Å for hump particles and $\mathrm{a} \in [6,\, 15]$ Å for PAH's (see Li & Greenberg 1997).

For the component of the small silicates resulting from the erosion of the silicate cores whose organic mantles have been completely removed, the size distribution is taken to be $\mathrm{n(a)} \sim \exp{[-5\,(\frac{\mathrm{a}}{\mathrm{a_j}})^2]}$, where $\mathrm{a}$, $\mathrm{a_j}$ are the silicate grain radius and the cut-off size of the distribution, respectively. The small silicate particles are also treated as infinite cylinders; i.e., assuming that they have some memory of the parental shape. This (shape assumption) does not significantly modify our results.

Finally, in fitting the extinction curve, there is only one free parameter left to be specified, i.e., $\mathrm{a_j}$ for the small silicate grains. Varying $\mathrm{a_j}$ and adjusting the relative number of each component, we find that $\mathrm{a_j} \approx 0.04\,\mu\mathrm{m}$ (corresponding to an average size of $<\mathrm{a}>\approx 0.01\,\mu\mathrm{m}$) provides a good fit to the observed extinction. Fig. 2 depicts the theoretical extinction curve calculated from the four-dust-component model from NIR to FUV

**Table 1.** Sizes and numbers of each dust component in the HD 210121 cloud. The dust-to-gas ratio is taken to be the same as the Galactic average value for the diffuse interstellar medium ($A_v/N_H \simeq 5.3 \times 10^{-22}\,\mathrm{mag\,cm^2}$, Bohlin et al. 1978). The elongation of “infinite cylinders” is denoted by $e$.

| | core-mantle | small silicate | hump | PAH’s |
|---|---|---|---|---|
| grain size | $n(a) \sim \exp\left[-5\left(\frac{a-a_c}{a_i}\right)^2\right]$ <br> $a_c = 0.042\,\mu m, a_i = 0.056\,\mu m$ | $n(a) \sim \exp\left[-5\left(\frac{a}{a_j}\right)^2\right]$ <br> $a_j = 0.040\,\mu m$ | $n(a) \sim a^{-3}$ <br> $a \in [15,\ 120]$ Å | $n(a) \sim a^{-3}$ <br> $a \in [6,\ 15]$ Å |
| $n_d/n_h$ | $\frac{\pi}{4e} \times 2.83 \times 10^{-12}$ | $\frac{\pi}{4e} \times 1.60 \times 10^{-10}$ | $1.69 \times 10^{-9}$ | $1.31 \times 10^{-6}$ |
| $n_d/n_{cm}$ | 1.00 | 57 | $\frac{4e}{\pi} \times 5.97 \times 10^2$ | $\frac{4e}{\pi} \times 4.63 \times 10^5$ |
| $m_d/m_{cm}$ | 1.00 | 1.34 | 0.12 | 0.37 |

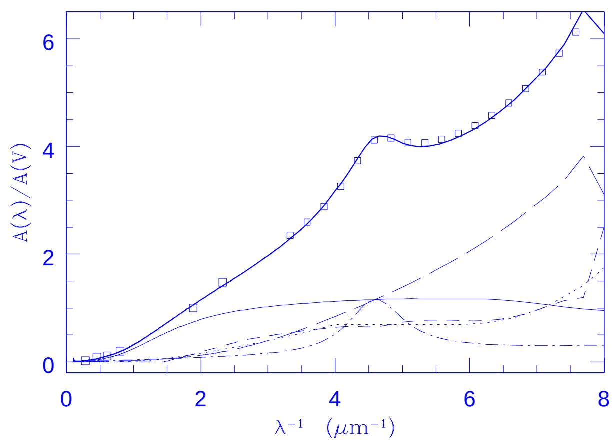


**Fig. 2.** The core-mantle model fits to the interstellar extinction curve of HD 210121. The observational data (Welty & Folwer 1992; Larson et al. 1996) are plotted as squares. Model results (thick solid line) are the sum of four dust components: core-mantle grains (thin solid); hump particles (dot-dashed); PAH’s (dotted); small silicates (long dashed). Also plotted is the residual PAH’s extinction (short dashed).

as well as the four individual contributions. The sudden drop at $\lambda^{-1} \approx 7.5\,\mu m^{-1}$ is caused by the sudden steep rise of the imaginary part $[m''(\lambda)]$ of the silicate complex refractive index $[m(\lambda) = m'(\lambda) - i\,m''(\lambda)]$. For detailed discussions we refer to Kim & Martin (1995). We do not see such a drop in the polarization curve or in the extinction curve from the core-mantle particles because the organic mantle masks the silicate core so that the sudden drop of $m''(\lambda)$ has been substantially diluted. Also plotted in Fig. 2 is the net decomposition PAH’s extinction contribution derived by subtracting the other three components (the core-mantle, the hump and the small silicate components) from the observation. Comparison of the calculated PAH’s extinction with the decomposition derived PAH’s extinction shows close agreement except at $\lambda^{-1} > 7.5\,\mu m^{-1}$. The visual polarization-to-extinction ratio is calculated to be $(P/A)_v \approx 0.187\,\mathrm{mag}^{-1}$. For finite cylinders this should be reduced by a factor of about 2, but it is still much higher than the observation $(P/A)_v \approx 0.0165\,\mathrm{mag}^{-1}$ (Larson et al. 1996). It is not surprising that our model overestimates $(P/A)_v$ because we have assumed not only perfect spinning alignment but also a completely perpendicular magnetic field in the calculations.

### *4.2. Elemental abundance constraints*

The adopted dust size parameters and the numbers of each dust component per hydrogen atom are summarized in Table 1. The mass ratio of the PAH’s component to the core-mantle particles is about three times that for the Galactic average. Such an overabundant PAH component could reasonably result from the erosion of the organic refractory mantles through grain-grain collisions or grain mantle explosions (Greenberg & Yencha 1973). To estimate the elongation $e$, we compare the infinite cylinder extinction curve with that calculated from volume-equivalent spherical core-mantle dust. It appears that spheres with volumes equivalent to infinite cylinders of $e = 4$ give arise to similar extinction results. We should note that, in Table 1, the dust-to-gas ratio is assumed to be the same as the Galactic average value for the diffuse interstellar medium ($A_v/N_H \simeq 5.3 \times 10^{-22}\,\mathrm{mag\,cm^2}$, Bohlin et al. 1978). From these numbers we can obtain the elemental depletion, another possible constraint on our dust model. Here special attention is given to silicon and carbon. Variations on the dust-to-gas ratio $A_v/N_H$ will be discussed later.

Assuming a mass density of $3.5\,\mathrm{g\,cm^{-3}}$, $1.8\,\mathrm{g\,cm^{-3}}$, and $2.3\,\mathrm{g\,cm^{-3}}$ for silicates, organic refractories, carbonaceous hump particles, respectively, we derive the total silicon depletion to be $\left[\frac{Si}{H}\right]_d \approx 43.6 \times 10^{-6}$ with $\left[\frac{Si}{H}\right]_d^{cm} \approx 12.6 \times 10^{-6}$ locked in the core-mantle grains and $\left[\frac{Si}{H}\right]_d^{si} \approx 31.0 \times 10^{-6}$ in the small silicate particles. However, the solar system silicon abundance is $\left[\frac{Si}{H}\right]_\odot \approx 36.0 \times 10^{-6}$ (Grevesse et al. 1996). If the interstellar abundance is that of the solar system, then it implies that our model needs about 20% more silicon than is available to condense into the solid phase. Similarly, the carbon depletion is estimated to be $\left[\frac{C}{H}\right]_d \approx 276 \times 10^{-6}$ with $\left[\frac{C}{H}\right]_d^{cm} \approx 110 \times 10^{-6}$ locked in the organic mantles, $\left[\frac{C}{H}\right]_d^{hump} \approx 39 \times 10^{-6}$ in hump particles and $\left[\frac{C}{H}\right]_d^{pah} \approx 123 \times 10^{-6}$ in PAH’s [derived from the residual PAH’s extinction (short-dashed line in Fig. 2)]. Recently, Cardelli et al. (1996) have analyzed the gas phase carbon abundance $\left[\frac{C}{H}\right]_g$ of six sight lines with the Goddard High Resolution Spectrograph (GHRS) aboard the Hubble Space Telescope. They found that the gas phase carbon abundance is invariant and environment independent, and is always $\left[\frac{C}{H}\right]_g \approx 140 \pm 20 \times 10^{-6}$. The environment independence is not easily explained. Snow et al. (1998) pointed out that these sight lines observed by Cardelli et al. (1996) are limited to diffuse cloud medium. If we adopt the value determined by Cardelli et al. (1996), our model requires a total carbon abundance of $\left[\frac{\rm C}{\rm H}\right] \approx 412 \times 10^{-6}$, about $15\%$ higher than the solar carbon abundance $\left[\frac{\rm C}{\rm H}\right]_\odot \approx 360 \times 10^{-6}$ [see Grevesse et al. 1996; but we should point out here that the actual solar carbon abundance may probably be higher than $360 \times 10^{-6}$; for example, in order to account for the comet coma abundances, Greenberg (1998) suggested a carbon to oxygen ratio $\rm C : O = 0.6$ which implies $\left[\frac{\rm C}{\rm H}\right]_\odot \approx 417 \times 10^{-6}$]. A recent study (Snow et al. 1998) shows that the gas phase carbon abundance in the translucent molecular cloud line of sight toward HD 24534 is only $\left[\frac{\rm C}{\rm H}\right]_{\rm g} \le 44 \times 10^{-6}$ which is much lower than the value suggested by Cardelli et al. (1996). Furthermore, the gas phase carbon abundance in IC 63, a reflection nebula, is only $\simeq 50 \times 10^{-6}$ (Jansen et al. 1996). Moreover, and in particular, on the basis of chemical modeling, Gredel et al. (1992) found that a gas phase abundance of $\left[\frac{\rm C}{\rm H}\right]_{\rm g} \approx 47 \times 10^{-6}$ for the HD 210121 cloud is consistent with the observed molecular abundances. If we adopt $\left[\frac{\rm C}{\rm H}\right]_{\rm g} \approx 47 \times 10^{-6}$ (Gredel et al. 1992), then the total carbon abundance is only $\left[\frac{\rm C}{\rm H}\right] \approx 323 \times 10^{-6}$, which is lower than the solar carbon abundance. For the sake of illustration, we list the relevant elemental abundances in Table 2.

## 5. The silicate/graphite model

The above discussions are based on the silicate core-organic refractory mantle model. For comparison, in this section we shall consider an alternative interstellar dust model: the bare silicate/graphite model (Mathis et al. 1977; Draine & Lee 1984).

In the framework of the silicate/graphite model, the interstellar extinction is a joint effort of bare silicate and graphite grains while the interstellar polarization is accounted for only by silicate grains because graphite is difficult to align. Following Mathis et al. (1977) and Draine & Lee (1984) and adopting the Draine & Lee (1984) optical constants of silicates and graphite, we first model the silicates and graphite as spherical grains with a power law size distribution $\rm n(a) \propto a^{-3.5}$. Adjusting the size ranges (both for silicates and for graphite), we find the best fit to the extinction curve is provided by $\rm a \in [0.001,\, 0.20]\,\mu m$ for silicates and $\rm a \in [0.001,\, 0.12]\,\mu m$ for graphite. As displayed in Fig. 3, the general match to the observation is acceptable except for the deviation in the region $\lambda^{-1} > 7.0\,\mu\rm m^{-1}$ which is relatively large.

Similarly, we calculate the elemental depletion. We find that the silicate/graphite model requires $\left[\frac{\rm Si}{\rm H}\right]_{\rm d} \approx 79.5 \times 10^{-6}$, an uncomfortablely high silicon abundance, being about twice the solar abundance. The carbon depletion is $\left[\frac{\rm C}{\rm H}\right]_{\rm d} \approx 195 \times 10^{-6}$. Adding up the gas phase carbon abundance, the silicate/graphite model indicates $\left[\frac{\rm C}{\rm H}\right] \approx 335 \times 10^{-6}$ ($\left[\frac{\rm C}{\rm H}\right]_{\rm g} \approx 140 \times 10^{-6}$, Cardelli et al. 1996) or $\left[\frac{\rm C}{\rm H}\right] \approx 242 \times 10^{-6}$ ($\left[\frac{\rm C}{\rm H}\right]_{\rm g} \approx 47 \times 10^{-6}$, Gredel et al. 1992), both of which are within the solar carbon abundance limit. The corresponding elemental abundances are also listed in Table 2.

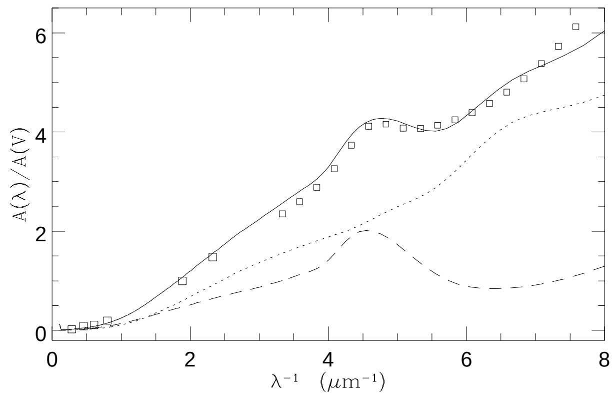


**Fig. 3.** The silicate/graphite model fits to the extinction curve of HD 210121. Squares are the observational data (Welty & Folwer 1992; Larson et al. 1996). Model results (solid line) are the sum of two dust components: silicates (dotted); graphite (dashed).

Although the silicate/graphite model can qualitatively reproduce the HD 210121 interstellar extinction observation, the required silicon abundance is unacceptably high. As can be seen in Fig. 3, a large amount of silicates are needed to account for the FUV extinction; as a matter of fact, the FUV extinction is dominated by silicates. On the other hand, the silicate/graphite model does not use up all the available carbon (at least within the solar abundance limit). This leads us to suggest a modified silicate/graphite model with an additional FUV component – PAH's included. We have attempted to fit the extinction curve in terms of the silicate/graphite+PAH's model using the UV properties of PAH's as represented by an analytical formula (Désert et al. 1990). No satisfactory fit can be obtained. This could be due to the uncertainty of the adopted PAH's UV properties. To put a strict interpretation on the failure of the silicate/graphite+PAH's model in fitting the extinction curve, appropriate experimental determinations of the UV cross sections as a function of wavelength are needed for a larger variety of PAH's of different sizes.

Here we are concerned primarily with the elemental abundances. So let us just estimate the carbon abundance required to be locked up in graphite and in PAH's. The silicon depletion is arbitrarily set at the solar abundance, $\left[\frac{\rm Si}{\rm H}\right]_{\rm d} \approx 36.0 \times 10^{-6}$. We keep the same amount of graphite as used in the silicate/graphite model since it is needed to provide the 2200 Å hump. We then extract the sum of graphite and silicate from the extinction curve and attribute the remaining extinction to PAH's. Note that the hump particles should not be expected to account for (even partially) the FUV rise (Greenberg & Chlewicki 1983). If we adopt the FUV absorption cross sections given by the formula of Désert et al. (1990) ($10^{-17}\,\rm cm^2$ per carbon atom at $\lambda^{-1} = 8.0\,\mu\rm m^{-1}$), the carbon abundance locked in PAH's is $\left[\frac{\rm C}{\rm H}\right]_{\rm d}^{\rm pah} \approx 136 \times 10^{-6}$. The total carbon depletion is then $\left[\frac{\rm C}{\rm H}\right]_{\rm d} \approx 331 \times 10^{-6}$. If the gas phase carbon abundance is $\left[\frac{\rm C}{\rm H}\right]_{\rm g} \approx 47 \times 10^{-6}$ as suggested by Gredel et al. (1992), then the silicate/graphite+PAH's model needs only $\left[\frac{\rm C}{\rm H}\right] \approx 378 \times 10^{-6}$, well within the uncertainty of the solar carbon abundance $\left[\frac{\rm C}{\rm H}\right]_\odot \approx 360 \times 10^{-6}$. However, if the gas

**Table 2.** The elemental depletion and cosmic abundance constraint (in unit of atoms per $10^6$ hydrogen nuclei).

| element x | | Si | C |
|---|---|---|---|
| cosmic abundance $\left[\frac{\mathrm{x}}{\mathrm{H}}\right]_{\mathrm{c}}$ | | 36.0$^{\dagger}$, 24.0$^{\ddagger}$ | 355$^{\dagger}$, 237$^{\ddagger}$ |
| core-mantle model | core | 12.6 | - |
| | mantle | - | 110 |
| | silicates | 31.0 | - |
| | hump | - | 39 |
| | PAH | - | 123 |
| | $\left[\frac{\mathrm{x}}{\mathrm{H}}\right]_{\mathrm{d}}$ | 43.6 | 276 |
| | $\left[\frac{\mathrm{x}}{\mathrm{H}}\right]_{\mathrm{d+g}}$ | 43.6$^{\oplus}$ | 412$^{\star}$, 323$^{*}$ |
| silicate/graphite model | silicate | 79.5 | - |
| | graphite | - | 195 |
| | $\left[\frac{\mathrm{x}}{\mathrm{H}}\right]_{\mathrm{d}}$ | 79.5 | 195 |
| | $\left[\frac{\mathrm{x}}{\mathrm{H}}\right]_{\mathrm{d+g}}$ | 79.5$^{\oplus}$ | 335$^{\star}$, 242$^{*}$ |
| silicate/graphite + PAH model | silicate | 36.0 | - |
| | graphite | - | 195 |
| | PAH | - | 136 |
| | $\left[\frac{\mathrm{x}}{\mathrm{H}}\right]_{\mathrm{d}}$ | 36.0 | 331 |
| | $\left[\frac{\mathrm{x}}{\mathrm{H}}\right]_{\mathrm{d+g}}$ | 36.0$^{\oplus}$ | 471$^{\star}$, 378$^{*}$ |

$^{\dagger}$ This "reference abundance" (the cosmic abundance $\left[\frac{\mathrm{x}}{\mathrm{H}}\right]_{\mathrm{c}}$) is assumed to be that of the solar system (Grevesse et al. 1996).
$^{\ddagger}$ This "reference abundance" is assumed to be $2/3$ of the solar system abundance (Grevesse et al. 1996).
$\oplus$ Assuming very low gas phase abundance for Si.
$^{\star}$ This gas phase carbon abundance is taken as $\left[\frac{\mathrm{C}}{\mathrm{H}}\right]_{\mathrm{g}} \approx 140 \times 10^{-6}$ (Cardelli et al. 1996).
$^{*}$ This gas phase carbon abundance is taken as $\left[\frac{\mathrm{C}}{\mathrm{H}}\right]_{\mathrm{g}} \approx 47 \times 10^{-6}$ (Gredel et al. 1992).

phase carbon abundance is $\left[\frac{\mathrm{C}}{\mathrm{H}}\right]_{\mathrm{g}} \approx 140 \times 10^{-6}$ as argued by Cardelli et al. (1996), then the silicate/graphite+PAH's model needs $\left[\frac{\mathrm{C}}{\mathrm{H}}\right] \approx 471 \times 10^{-6}$, which is again much higher than the solar carbon abundance. The elemental depletion for this model is also presented in Table 2.

## 6. Emission

Dust grains absorb stellar UV/visual photons and reradiate them at longer wavelengths. Apart from the extinction and polarization observational constraints, the IR emission comparison of the measurements with the model predictions permits further tests of dust models and also provides information on the interstellar radiation field which is needed in interstellar cloud chemical modeling (see e.g. van Dishoeck 1994). In this section we will concentrate on the four-component core-mantle model and only with a brief discussion on the silicate/graphite model.

The temperatures of the core-mantle grains ($< \mathrm{a} >= 0.056\,\mu\mathrm{m}$) and the small silicate particles ($< \mathrm{a} >= 0.01\,\mu\mathrm{m}$) can be determined on the basis of the energy balance between absorption and emission. On the other hand for hump particles and PAH's, since their heat contents are comparable to or smaller than the energy of an interstellar UV photon (photon absorptions are infrequent), they cannot reach steady-state temperatures; instead, they would undergo temperature fluctuations (Greenberg 1968). In calculating grain temperatures or temperature fluctuations, we need to know the interstellar radiation field (ISRF). For the solar neighborhood, van Dishoeck (1994) has summarized several typical ISRF estimates (see her Fig. 2). For high latitude clouds, the ISRF would be relatively weak due to the deficiency of nearby early-type stars as well as being about $150\,\mathrm{pc}$ away from the Galactic plane. Indeed, the relatively high molecular abundances with respect to the low visual extinction in the cloud are shown to be indicative of a low ISRF (de Vries & van Dishoeck 1988; Gredel et al. 1992; Stark & van Dishoeck 1994). We adopt the general wavelength distribution of solar neighborhood ISRF as compiled by Mathis et al. (1983) but, following van Dishoeck & Black (1989), scale the ISRF by a constant $\mathrm{I_{uv}}$, without taking into account the hardness/softness modifications. With the excess UV dust extinction, the penetration within the cloud is substantially less than for an equal visual extinction in the Galactic plane.

For the purpose of calculating dust FIR emission, we represent the infinite cylinders (elongation $\mathrm{e} = 4$) by equal-volume spheres of which the extinction curve is similar to that of the infinite cylinders. For a given $\mathrm{I_{uv}}$, the temperatures of the core-mantle grains as a function of dust size are derived by equating the absorbed and emitted energy. The emission is then integrated over the whole dust size distribution. The steady-state temperatures are also calculated for the equal-volume spherical counterparts of the small silicate particles as a function of grain size. In the fully extended size range of smaller silicate grains, temperature fluctuations need to be considered, but note that those transiently heated particles take up only a very small fraction in the size distribution and make a negligible contribution to the emission. The elongation of the small silicate infinite cylinders is chosen as $\mathrm{e} = 4$ (same as their parental grains) because their extinction curve is also well represented by the corresponding equal-volume spheres. While $\mathrm{e} = 5$ gives the best representation, there is almost no difference in the resulting emission spectrum between $\mathrm{e} = 5$ and $\mathrm{e} = 4$. The equilibrium temperatures for the mean size core-mantle grains ($< \mathrm{a} >= 0.056\,\mu\mathrm{m}$) are about 19.6 K, 17.5 K, 16.4 K and 15.6 K for $\mathrm{I_{uv}} = 1, 1/2, 1/3, 1/4$, respectively. For the small silicate particles, the mean size ($< \mathrm{a} >= 0.01\,\mu\mathrm{m}$) equilibrium temperatures are about 18.0 K, 16.0 K, 15.0 K and 14.3 K for $\mathrm{I_{uv}} = 1, 1/2, 1/3, 1/4$, respectively. Note the resulting emission is always the integration over the whole dust size distribution. For the hump particles and PAH's, we use the relatively simple method described in Aannestad (1989) to calculate the temperature distribution probabilities as a function of grain size. The enthalpy of graphite (Chase et al. 1985) is used for hump particles and the approximate formula given by Léger & d'Hendecourt (1987) is used for PAH's. The emission from hump particles or PAH's is obtained by integrating over the temperature distribution and over the grain size distribution. The resulting emission spectrum is a sum for all four dust components. For simplicity, we have not considered the cloud depth-dependence as was done in the chemical modeling efforts (see e.g., de Vries & van Dishoeck 1988; Gredel et al. 1992; Stark & van Dishoeck 1994); instead, we treat the entire cloud as illuminated homogeneously by the $I_{uv}$-scaled ISRF.

In Fig. 4 we present the dust emission spectra calculated from $I_{uv} = 1, 1/2, 1/3, 1/4$. Also plotted is the IRAS $12\,\mu$m, $25\,\mu$m, $60\,\mu$m and $100\,\mu$m data (Welty & Fowler 1992). It can be clearly seen that the IRAS data are best matched by $I_{uv} = 1/3$. This is consistent with the earlier determinations (de Vries & van Dishoeck 1988; Gredel et al. 1992; Stark & van Dishoeck 1994) which suggest that the ISRF incident on the HD 210121 cloud surface may be only half of the diffuse interstellar medium ($I_{uv} = 1/2$). Note the ISRF (scaled by $I_{uv} = 1/3$) used in this work is for the whole cloud, rather than the ISRF incident on the cloud surface. A weaker ISRF is also in agreement with the lower ratio of the IRAS $100\,\mu$m intensity to the hydrogen column density $I(100\,\mu m)/N_H = 0.34\,M\,Jy\,sr^{-1}(10^{20}\,cm^{-2})^{-1}$ (Welty & Fowler 1992) than that for the diffuse interstellar medium $I(100\,\mu m)/N_H = 0.87\,M\,Jy\,sr^{-1}(10^{20}\,cm^{-2})^{-1}$. Dust IR emission measurements at much longer wavelength ($135\,\mu$m, $160\,\mu$m, $180\,\mu$m and $200\,\mu$m) have been performed by ISO and the data reduction and analysis are in progress (Stark et al., in preparation). We expect that the ISO data will provide a powerful test of our dust model and on the conclusion reached for the ISRF.

We did not perform new calculations of the FIR emission for the silicate/graphite model. However, we expect that similar results on the radiation field will also be obtained for the silicate/graphite model. Compared to the Galactic average, the HD 210121 cloud dust grains in the silicate/graphite model are relatively smaller (see Sect. 5). If the radiation field were the same as in the Galactic plane, then the dust grains would be hotter and the corresponding emission spectrum would peak at a shorter wavelength than for the Galactic average. The preliminary analysis of the ISO data shows that the HD 210121 cloud spectrum peaks at $\sim 160\,\mu$m (Stark et al., in preparation) which is longer than that of the general diffuse interstellar medium ($\sim 140\,\mu$m). Our model spectrum ($I_{uv} = 1/3$) peaks at $\sim 150\,\mu$m. In general, the silicate/graphite mixtures are somewhat hotter than the core-mantle particles (see Fig. 4 in Greenberg & Li 1996), thus the emission spectrum predicted from the silicate/graphite model for $I_{uv} = 1/3$ would peak at a wavelength even shorter than $\sim 150\,\mu$m. Therefore the silicate/graphite model also leads to a weaker ISRF.

## 7. Discussion

The relatively high molecular abundances per unit visual extinction ($A_v$) for the line of sight toward HD 210121 can be readily understood in terms of its peculiar dust properties and the incident radiation field. First of all, the unusually steep FUV

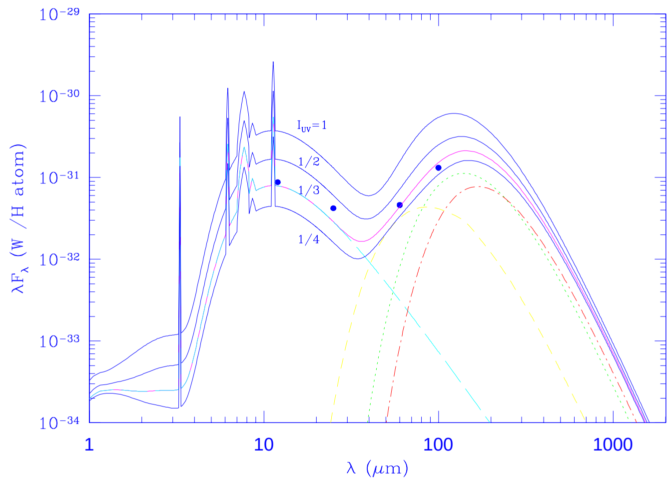


**Fig. 4.** Fits of the emission by the core-mantle model with various radiation field intensities (solid lines; from top to down: $I_{uv} = 1, 1/2, 1/3, 1/4$) to the IRAS data (points; Welty & Fowler 1992). Also plotted are the contributions from each dust component: core-mantle particles (dotted); PAH's (long dashed); hump particles (dashed); small silicates (dot-dashed).

extinction leads to rapid attenuation of UV photons (per unit visual extinction) and thus decreased molecular photodissociation rates. Indeed, observations have shown that $H_2$, CH and CN are enhanced in lines of sight characterized by steeper FUV extinction (Cardelli 1988). Van Dishoeck & Black (1989) have theoretically demonstrated that higher UV extinction leads to higher CO, CN abundances. Furthermore, the anomalously large amount of small particles provide an exceptionally large grain surface area for molecular formation. Moreover, the relatively weak UV radiation field provides a less harsh environment for survival of molecules.

While the abundances of the molecular species in the HLC toward HD 210121 ($A_v \approx 1.0$ mag) are enhanced compared with the classical diffuse cloud $\zeta$ Oph of comparable visual extinction ($A_v \approx 0.9$ mag), the $CH^+$ abundance, which is commonly considered as a signature of shock processes, is relatively low (de Vries & van Dishoeck 1988). [However, it is interesting to note that a correlation between the $12\,\mu$m emission (indicative of very small particles) and the $CH^+$ abundance was reported for some lines of sight by Boulanger (1994).] In addition, Welty & Fowler (1992) found that the calcium and titanium depletions for this line of sight are within the normal range for moderately dense diffuse clouds. Furthermore, the CO velocity is almost constant across the cloud (Gredel et al. 1992). All these seem to rule out substantial *current* grain destruction and the *recent* occurrence of strong shocks in the cloud. Thus the presence of a large amount of small particles cannot be interpreted in terms of destruction mechanisms such as sputtering, or shattering due to shock-driven grain-grain collisions *currently* taking place in the cloud. Larson et al. (1996) attributed it to a lack of growth by coagulation of the small to medium-sized grains. This is questionable because, compared to the diffuse interstellar medium, one may expect a more efficient grain-grain coagulation in the

HD 210121 cloud where there are no strong shocks and a less intense radiation field. The model proposed here is more favorable since we assume that the core-mantle grains have been *earlier* eroded somewhere in their paths to high latitudes rather than directly in the cloud. We have not explored here in detail how dust and gas are transferred to high latitudes but just assign it to some sort of cloud photolevitation, Galactic fountain or turbulence.

Recently, it has been suggested that the elemental abundance of the interstellar medium is perhaps only 2/3 of the solar abundance (see e.g., Snow & Witt 1996). With such reduced abundances, all attempts to fit the average Galactic extinction curve face the problem of insufficient carbon (Mathis 1996; Li & Greenberg 1997). If the interstellar abundance is really subsolar, the depletion problem imposed on the HD 210121 cloud dust (both for the core-mantle model and for the silicate/graphite model) is even more serious because, there would be only $\left[\frac{\mathrm{C}}{\mathrm{H}}\right]_{\mathrm{d}} \approx 355 \times 10^{-6} \times 2/3 - 140 \times 10^{-6} = 97 \times 10^{-6}$ (Cardelli et al. 1996) or $\left[\frac{\mathrm{C}}{\mathrm{H}}\right]_{\mathrm{d}} \approx 355 \times 10^{-6} \times 2/3 - 47 \times 10^{-6} = 190 \times 10^{-6}$ (Gredel et al. 1992) carbon and $\left[\frac{\mathrm{Si}}{\mathrm{H}}\right]_{\mathrm{d}} \approx 36 \times 10^{-6} \times 2/3 = 24 \times 10^{-6}$ silicon available for depletion in dust.

Even with the solar abundance, there is clearly a silicon budget crisis for the silicate/graphite model (see Sect. 5 and Table 2). However with the inclusion of a PAH's component, the silicate/graphite model seems to be reasonably consistent with the solar abundance (if $\left[\frac{\mathrm{C}}{\mathrm{H}}\right]_{\mathrm{g}} \approx 47 \times 10^{-6}$ as proposed by Gredel et al. 1992). For the core-mantle model, the best fitting case requires a bit more silicon ($\approx 20\%$) than the solar silicon abundance. If the gas phase carbon abundance is $\left[\frac{\mathrm{C}}{\mathrm{H}}\right]_{\mathrm{g}} \approx 140 \times 10^{-6}$ (Cardelli et al. 1996), the core-mantle model consumes $\approx 15\%$ more carbon than the solar abundance. Note that the above discussions on the elemental depletions are made on the basis of the adoption of the canonical dust/gas ratio $\mathrm{A_v/N_H} \simeq 5.3 \times 10^{-22}\,\mathrm{mag\,cm^2}$ which is valid for the Galactic average. It is not clear a priori that the Galactic average dust/gas ratio also applies to the high-latitude clouds.

Thus one possible solution to the abundance problem may lie in the existence of a lower dust/gas ratio in the HLC toward HD 210121 as is the case for some dark cloud lines of sight (Kim & Martin 1996) and the high latitude cloud MBM 18 (Penprase et al. 1990). If the dust/gas ratio is $\approx 20\%$ lower than that of the general interstellar medium ($\mathrm{A_v/N_H} \simeq 5.3 \times 10^{-22}\,\mathrm{mag\,cm^2}$) adopted here, then the core-mantle model is in good agreement with the solar abundance. As a matter of fact, Larson et al. (1996) estimated the total to selective extinction ratio $\mathrm{R_v} \approx 2.1 \pm 0.2$ and the color excess $\mathrm{E_{B-V}} \approx 0.38$, giving the visual extinction $\mathrm{A_v} \approx 0.8 \pm 0.09$; the total hydrogen column density [$\mathrm{N_H} = \mathrm{N(H)} + 2\,\mathrm{N(H_2)}$] was estimated to be $\mathrm{N_H} \approx 1.9 \times 10^{21}\,\mathrm{cm^{-2}}$ [the molecular hydrogen column density $\mathrm{N(H_2)} \approx (8 \pm 2) \times 10^{20}\,\mathrm{cm^{-2}}$ (de Vries & van Dishoeck 1988); the atomic hydrogen column density $\mathrm{N(H)} \approx 2.9 \times 10^{20}\,\mathrm{cm^{-2}}$ (Welty & Fowler 1992)]; therefore, the dust/gas ratio becomes $\mathrm{A_v/N_H} \simeq 4.2 \times 10^{-22}\,\mathrm{mag\,cm^2}$, which is about 20% lower than the general value $\mathrm{A_v/N_H} \simeq 5.3 \times 10^{-22}\,\mathrm{mag\,cm^2}$!

However, one should keep in mind that there is a considerable scatter in the estimation of the molecular hydrogen column density $\mathrm{N(H_2)}$ (de Vries & van Dishoeck 1988). At this moment one can not rule out the possibility of a much lower column density. As discussed in de Vries & van Dishoeck (1988), a small $\mathrm{H_2/CO}$ conversion factor would lead to $\mathrm{N(H_2)} \approx 2 \times 10^{20}\,\mathrm{cm^{-2}}$, while the other $\mathrm{N(H_2)}$ numbers which are much higher could be overestimated by adopting $\mathrm{R_v} = 3.1$ or by using the $\mathrm{CH/H_2}$ abundance correlation without taking into account the different physical conditions (e.g. the radiation field). Therefore, it may also be possible that the dust/gas ratio in the high-latitude cloud toward HD 210121 is actually higher than in the Galactic plane; namely, the extinction (thus also the total amount of dust grains) per unit mass of gas material is higher. This implies that there is a relatively larger amount of condensed atoms (e.g. C, O, Si, Mg, Fe etc.) per H atom than in the Galactic plane. In the context of this scenario, it can be understood why the core-mantle model for the high-latitude cloud needs a much higher silicon and carbon depletion than for the Galactic average ($\left[\frac{\mathrm{Si}}{\mathrm{H}}\right]_{\mathrm{d}} \approx 20 \times 10^{-6}$, $\left[\frac{\mathrm{C}}{\mathrm{H}}\right]_{\mathrm{d}} \approx 194 \times 10^{-6}$, see Li & Greenberg 1997).

On the other hand, if the gas phase carbon abundance is $\left[\frac{\mathrm{C}}{\mathrm{H}}\right]_{\mathrm{g}} \approx 47 \times 10^{-6}$ (Gredel et al. 1992), it implies that there is still some carbon left to be included in the core-mantle model. If we set the small silicates at $\left[\frac{\mathrm{Si}}{\mathrm{H}}\right]_{\mathrm{d}} \approx 23.4 \times 10^{-6}$ so that the total silicon abundance is $36 \times 10^{-6} \approx \left[\frac{\mathrm{Si}}{\mathrm{H}}\right]_{\odot}$, and attribute the remaining FUV extinction to be accounted for by PAH's, then we need $\left[\frac{\mathrm{C}}{\mathrm{H}}\right]_{\mathrm{d}}^{\mathrm{pah}} \approx 160 \times 10^{-6}$ and the total carbon depletion is $\left[\frac{\mathrm{C}}{\mathrm{H}}\right]_{\mathrm{d}} \approx 309 \times 10^{-6}$. Thus the dust plus gas carbon abundance is $\left[\frac{\mathrm{C}}{\mathrm{H}}\right]_{\mathrm{d}} \approx 356 \times 10^{-6}$, closely consistent with the solar abundance.

We also need to note that the adopted mass density $3.5\,\mathrm{g\,cm^{-3}}$, and $1.8\,\mathrm{g\,cm^{-3}}$ for silicates and organic refractories, respectively, may be overestimated. It may be more reasonable to assume a lower mass density for silicates and organic refractories. As a matter of fact, the density of terrestrial silicates could be as low as $2.5\,\mathrm{g\,cm^{-3}}$. If this is indeed the case, the corresponding abundances required to be locked up in dust grains as listed in Table 2 would be lower.

Because of the uncertainties remaining in the constraints on the high-latitude cloud dust and gas composition it is difficult to be dogmatic about what we can infer from the depletion. We believe that among the suggestions above, the most reasonable one is that the dust/gas ratio is actually higher than the Galactic average and that the extra silicon abundance relative to the solar system is consistent with the fractionation produced by having more dust relative to hydrogen as a result of the selective ejection of the dust outward from the plane.

Finally, we note that the HD 210121 cloud sight line is not a unique case. Many other lines of sight also exhibit a steeper FUV extinction than the average one (see Cardelli et al. 1989 and references therein). The physical conditions of these lines of sight could be generally different from that of diffuse interstellar medium. Their steeper FUV extinction may be attributed to a smaller average grain size (thinner mantle) and/or an enhanced abundance of FUV particles (PAHs) or even the presence of an extra component of small silicate grains just as inferred for the line of sight to the HD 210121 cloud.

## 8. Conclusion

We have modeled the interstellar extinction, polarization and emission in the high-latitude cloud toward HD 210121 within the framework of the core-mantle interstellar dust model. The dust content in this line of sight HLC has been assumed to have originated from the Galactic plane via either a violent energetic explosion process ("Galactic fountain"), or the relatively gentle "photolevitation", or some combination mechanism. The core-mantle grains have been partially eroded and thus have a thinner organic refractory mantle. In addition to the classical core-mantle particles, hump particles and PAH's, an extra component of small silicates resulting from the destruction (shattering, fragmentation) of the core-mantle particles is included to account for the FUV extinction together with PAH's. The polarization curve, characteristic of smaller grain size than the Galactic average, is well fitted by the core-mantle particles with smaller mantles than those in the Galactic plane. Thanks to the small silicate component, the extinction curve, characterized by an extremely steep FUV rise, is matched by the four-component core-mantle dust model. The corresponding elemental depletion is consistent with the solar abundance. We have also modeled the dust IR emission spectrum. Comparison of the model calculation with the IRAS data shows that the radiation field in this high-latitude cloud line of sight is about $1/3$ of the average interstellar radiation field, qualitatively in agreement with the earlier chemical modeling efforts. For the sake of comparison, we have also modeled the extinction in terms of the silicate/graphite model. It turns out that the silicate/graphite model is also able to give a good fit to the extinction curve, but it requires an unrealistically high silicon depletion to account for the FUV extinction. With an additional component, PAH's, included in the silicate/graphite model, the elemental depletion is consistent with the solar abundance constraint. If the interstellar medium abundance is subsolar (say, only $2/3$ of the solar abundance) as proposed more than two decades ago (Greenberg 1974) and recently discussed with much interest, both the core-mantle model and the silicate/graphite+PAH's model would face the problem of an abundance budget crisis.

*Acknowledgements.* We are grateful for the support by NASA grant NGR 33-018-148 and by a grant from the Netherlands Organization for Space Research (SRON). We thank Prof. W.B. Burton, Prof. E.F. van Dishoeck and Dr. W.A. Schutte for their useful suggestions. One of us (AL) wishes to thank Leiden University for an AIO fellowship and the World Laboratory for a scholarship and the National Science Foundation of China for financial support. We also thank the referee for some helpful suggestions.

## References

Aannestad, P.A., 1989, in: Evolution of Interstellar Dust and Related Topics, Bonetti, A., Greenberg, J.M., & Aiello, S. (eds.), Amsterdam, North Holland, p. 121
Allamandola, L.J., Tielens, A.G.G.M & Barker, J.R., 1989, ApJS 71, 733
Bohlin, R.C., Savage, B.D. & Drake, J.F., 1978, ApJ 224, 132
Boulanger, F., 1994, in: The Infrared Cirrus and Diffuse Interstellar Clouds, Cutri, R. & Latters, W.B. (eds.), San Francisco, ASP Conference Series 58, p. 101
Cardelli, J.A., 1988, ApJ 335, 177
Cardelli, J.A., Meyer, D.N., Jura, M. & Savage, B.D., 1996, ApJ, 467, 334
Chase, M.W., Davis, C.A., Downey, J.R. et al., 1985, J. Phys. Chem. Ref. Data, 14, Suppl. No.1
de Vaucouleurs, G. & Buta, R., 1983, AJ 88, 939
de Vries, C.P. & van Dishoeck, E.F., 1988, A&A 203, L23
Désert, F.X., Bazell, D. & Boulanger, F., 1988, ApJ 334, 815
Désert, F.X., Boulanger, F. & Puget, J.L., 1990, A&A 237, 215
Deul, E.R. & Burton, W.B., 1992, Chapter 5 of Burton, W.B., Distribution and observational properties of the interstellar medium, in: The Galactic Interstellar Medium, Burton, W.B., Elmegreen, B.G. & Genzel, R. (eds.), Springer, Berlin, p. 81
Draine, B.T. & Lee, H.M., 1984, ApJ 285, 89
Dwek, E., Arendt, R.G., Fixsen, D.J., et al., 1997, ApJ, 475, 565
Fitzpatrick, E.L. & Massa, D., 1986, ApJ 307, 286
Franco, J., Ferrini, F., Ferrara, A. & Barsella, B., 1991, ApJ 366, 443
Gredel, R., van Dishoeck, E.F., de Vries, C.P. & Black, J.H., 1992, A&A 257, 245
Greenberg, J.M., 1968, in: Stars and Stellar Systems, Vol. VII, Middlehurst, B.M. & Aller, L.H. (eds.), University of Chicago Press, p. 221
Greenberg, J.M. & Yencha, A.J., 973, in: IAU Symposium 52, Interstellar Dust and Related Topics, Greenberg, J.M. & van de Hulst, H.C. (eds.), Reidel, p. 369
Greenberg, J.M. 1974, ApJ 189, L81
Greenberg, J.M., 1978, in: Cosmic Dust, McDonnell, J.A.M. (ed.), Wiley, p. 187
Greenberg, J.M. & Chlewicki, G., 1983, ApJ 272, 563
Greenberg, J.M. & Li, A., 1996, in: New Extragalactic Perspectives in the New South Africa, Block, D.L. & Greenberg, J.M. (eds.), Kluwer, p. 118
Greenberg, J.M., 1998, A&A 330, 375
Grevesse, N., Noels, A. & Sauval, A.J., 1996, in: Cosmic Abundances, Holt, S.S. & Sonneborn, G. (eds.), ASP Conf. Series, Vol. 99, p. 117
Heiles, C. & Habing, H.J., 1974, A&AS 14, 1
Hong, S.S. & Greenberg, J.M., 1980, A&A 88, 194
Jansen, D.J., van Dishoeck, E.F., Keene, J.B., Boreiko, R. & Betz, A.L., 1996, A&A 309, 899
Joblin, C., Léger, A. & Martin, P., 1992, ApJ 393, L79
Kim, S.H. & Martin, P.G., 1995, ApJ 442, 172
Kim, S.H. & Martin, P.G., 1996, ApJ 462, 296
Larson, K.A., Whittet, D.C.B. & Hough, J.H., 1996, ApJ 472, 755
Léger, A. & d'Hendecourt, L., 1987, in: Polycyclic Aromatic Hydrocarbon and Astrophysics, Léger, A., et al. (eds.), p. 223
Li, A. & Greenberg, J.M., 1997, A&A 323, 566
Mathis, J.S., Rumpl, W. & Nordsieck, K.H., 1977, ApJ 217, 425
Mathis, J.S., Mezger, P.G. & Panagia, N., 1983, A&A, 128, 212
Mathis, J.S., 1996, ApJ 472, 643
Mennella, V., Colangeli, L., Palumbo, P., et al., 1996, ApJ 464, L91

Penprase, B.E., Blades, J.C., Danks, A.C. & Crane, P., 1990, ApJ 365, 241
Rouleau, F., Henning, Th. & Stognienko, R., 1997, A&A 322, 633
Schnaiter, M., Mutschke, H., Dorschner, J., Henning, Th. & Salama, F., 1998, ApJ 498, 486
Shane, C.D. & Wirtanen, C.A., 1967, The distribution of galaxies, Pub. Lick Obs. 22, Part I
Snow, T.P. & Witt, A.N., 1996, ApJ 468, L65
Snow, T.P., Black, J.H., van Dishoeck, E.F., et al., 1998, ApJ 496, L113
Stark, R. & van Dishoeck, E.F., 1994, A&A 286, L43
Stark, R., Laureijs, R.J., van Dishoeck, E.F., et al., 1998, in preparation
van Dishoeck, E.F. & Black, J.H., 1988, ApJ 334, 371
van Dishoeck, E.F. & Black, J.H., 1989, ApJ 340, 273
van Dishoeck, E.F., Black, J.H., Phillips, T.G. & Gredel, R., 1991, ApJ 366, 141
van Dishoeck, E.F., 1994, in: The Infrared Cirrus and Diffuse Interstellar Clouds, Cutri, R. & Latters, W.B. (eds.), San Francisco, ASP Conference Series 58, p. 319
Welty, D.E. & Fowler, J.R., 1992, ApJ 393, 193